Application of Evolution Algorithms to Aluminium Alloy Casting Porosity Prediction Function

Natnapat Gaviphatt[1,a], Prabhas Chongstitvatana[1,b] and Chedtha Puncreobutr[2,c]

[1]Department of Computer Engineering, Chulalongkorn University,
Phayathai Road, Pathumwan, Bangkok, 10330, Thailand

[2] Department of Metallurgical Engineering, Chulalongkorn University,
Phayathai Road, Pathumwan, Bangkok, 10330, Thailand

[a]natnapat.g@student.chula.ac.th, [b]prabhas.c@chula.ac.th, [c]chedtha.p@chula.ac.th

Keywords: Genetic algorithm, Differential evolution, Porosity, Aluminium alloys

Abstract. Porosity is a major problem occurring in aluminium alloy casting. During the process of solidification, alloy would shrink and emit dissolving hydrogen causing porosity formation inside the solidified part which leads to mechanical properties degradation. This research aims to produce a formula to explain the resulting porosity with the initial chemical compositions and cooling rate. A mathematic model is, at first, inferred from previous researches to be a template function. Evolution Algorithms are utilized to generate inner polynomial parts and to find appropriate coefficients to fit the experimental data obtained from publications. The optimized function promisingly shows good fit to the problem domain demonstrating that the resulting function is an effective model to explain porosity formation behaviour.

Introduction

In the last few decades, aluminium has turned into an extremely popular metallic material especially its casting alloys. Porosity formation from casting process is one of the major problems since it can limit elongation and fatigue properties of the final product [1]. For the last few decades, there are many researches related to explanation or prediction of porosity formation in Al casting ranging from analytical models and chemical and thermodynamic relations to computer simulations of casting process that are able to predict formation of macroporosity precisely [2-4]. However, for microporosity, most models still have some limitations and are unable to overcome conditions found in industrial castings. Recently artificial neural networks (ANN) are applied to porosity prediction [5, 6] which provided satisfactorily accurate predictive frameworks. Nevertheless, the models acquired from ANN training processes could be difficult to analyze the influences of variables.

This study aims to create a formula to explain the tendency of porosity amount with chemical compositions and cooling rate as independent variables. Model of function is derived from [6] to leave only polynomial parts to be operated. The function is optimized to fit experimental data from Dash and Makhlouf [7] with utilization of genetic algorithm and differential evolution.

Methodology

Porosity formation — Porosity in aluminium casting alloy could be classified, by causes, into 2 main types [8]. The first one is shrinkage porosity which rises from significantly lower volume of solid alloy compare to what it is in liquid state. In other words, when alloy liquid goes through solidification process, shrinkage occurs. Without adequate feeding and pressure, it is certain to leave undesirable empty space. The other one is gas porosity. This type of porosity happens from solvent's ability to dissolve gases (hydrogen in particular for Al alloys) and the loss of alloy after it solidified resulting in emission of hydrogen gas to surrounding liquid.

Template Function — According to [6], each hydrogen porosity and shrinkage porosity relies on a certain trend. For hydrogen porosity, the faster cooling proceeds, the less time for gas to diffuse toward pores. In other words, porosity should decrease with the higher cooling rate. To imitate the trend, the exponential decay function, Eq. 1, is the most suitable since it would not go below zero.

$$f(x) = c_1 e^{-c_2 x} \tag{1}$$

The shrinkage porosity, however, inclines in the opposite way since quick solidification can cause more formation of dendrites which resist the feeding flow and lead to formation of shrinkage porosity. Exponential growth function is actually applicable. Accordingly, the logistic function, Eq. 2, possessing the same growing manner without exceeding limit, gains more favour in this case.

$$f(x) = \frac{c_1}{1 + c_2 e^{-c_3 x}} \tag{2}$$

In reality, both types of porosity should occur simultaneously. With a hypothesis of absolute independency between them, total porosity shall be the result of summing them up as in Eq. 3 where P_i are polynomials being responsible for adjusting the functions magnitudes and transformations and R is the cooling rate.

$$p\% = \frac{P_1}{e^{P_2 + P_3 R}} + \frac{P_4}{1 + e^{P_5 - P_6 R}} \tag{3}$$

Function Generation and Optimization — Genetic algorithm (GA) [9] is used in conjunction with Differential Evolution (DE) [10] to generate the suitable form of the equation and its parameters that fit to the experimental data. Powers of each variable are serialized into a string of integers to serve as a chromosome for GA as well as parameters that are turned into a vector for DE as shown in Fig. 1.

Fig. 2 demonstrates the flow of GA-DE to search for good fit polynomials of the function to experimental data. The process scheme is summarized, using the configurations in Table 1, as follow:

1. Randomly create the first generation of function's powers.
2. Repeat all of the following steps for GA in order until any termination criterion are satisfied.
3. Create a new generation of function powers by applying uniform recombination and uniform mutation.
4. Each of the new generated functions must search for its proper parameters by utilizing DE.
5. Once all of the functions in both population pool and offspring become aware of their relevant parameters, evaluate error of every single function and select only the best one to be the new generation.

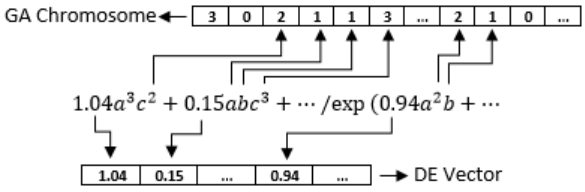

Figure 1 Representation model

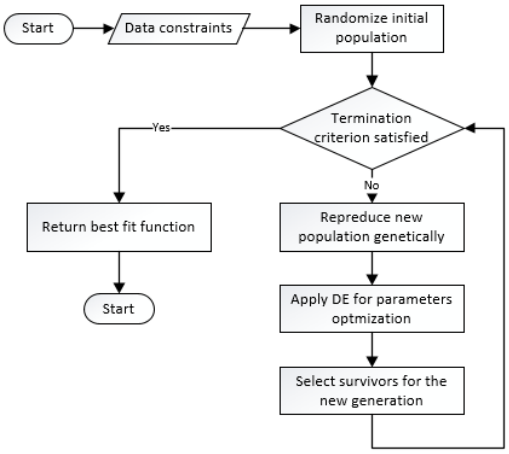

Figure 2 Flow chart of GA-DE method

Table 1 Algorithm configurations

GA configuration	DE configuration
Representation : Integer, μ = 250, λ=75	Population : μ = 200
Mutation : Uniform, p_m = 0.3	Scale Factor : F = 0.85
Recombination : Uniform	Crossover Probability : Cr = 0.75
Selection : Elitist	Strategy : DE/rand/1 either-or-algorithm

Experimental Data — The dataset used here is experimental data published by [7]. They provided 96 samples of porosity percent results along with the relevant chemical compositions consisting of silicon, iron, copper, magnesium, manganese, strontium and titanium. Moreover, cooling rates are also displayed which is the important reason why this dataset is chosen as a main model.

Results and Discussion

The best function obtained from GA-DE is presented below, Eq. 4.

$$p\% = \frac{2.57CuSr + 2.00SiSr + 0.001SiFe}{1 + 6.64e^{9.21Mg + 6.80Ti + 48.50FeMnTi - 0.73MgR - 2.45TiR}} + \frac{0.65 + 2.43Mn + 1.25Mg + 0.80Fe + 140.86MnSr}{e^{0.17R + 200FeMgMn^2Ti + 15.18Fe^2MgMn^2}} \quad (4)$$

Fig. 3 illustrates the accuracy of the presented function to predict the total porosity percent in aluminium casting. A very good agreement is found between the predicted values and the measured values of all 96 training data [7], as shown in Fig. 3a, with the root-mean-square error (RMSE) of 0.05. In addition, it can be clearly seen in Fig. 3b that the predicted porosity promisingly shows good fit to the measured porosity of 9 validation data reported by Dinnis *et al.* [11]. The RMSE of the regression is ~0.1.

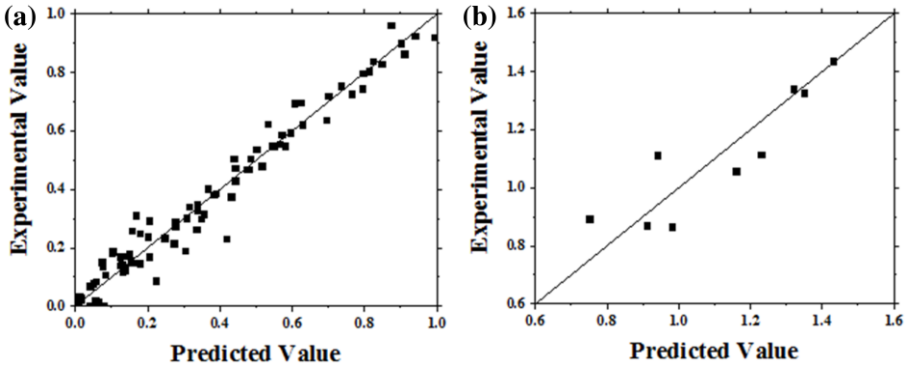

Figure 3 The predicted values of porosity percent compared with the experimental values reported by (a) Dash and Makhlouf [7] and (b) Dinnis *et al.* [11]

The prediction of total porosity as a function of cooling rate during solidification is depicted in Fig. 4. In the lower range of cooling rate (Fig. 4a), porosity decreases monotonically with greater cooling rate. It can be observed that porosity decreases substantially from ~1% to less than 0.5% when the cooling rate of 5.5 K/s is doubled. An increasing cooling rate would allow less time for hydrogen gas to diffuse towards the pores. As the growth of gas porosity is controlled by diffusion [3], this restriction inhibits the formation of gas porosity and thus leading to the reduction of total porosity. Similar phenomena have been reported in previous studies [12, 13].

In the higher range of cooling rate (Fig. 4b), the volume fraction of porosity, on average, is significantly lower than that in the lower cooling rate range. Note the different scales in Fig.4a and Fig. 4b. Unlike the lower range, the total porosity is observed to increase with increasing cooling rate. Although an increasing cooling rate would decrease the amount of gas porosity as discussed earlier, the formation of shrinkage porosity is more pronounced in this range of fast cooling [14]. The rapid solidification causes a smaller secondary dendrite arm spacing (SDAS) which is attributes to the

corresponding decrease in permeability. This will attribute to larger pressure drop and hence higher shrinkage porosity [6, 15]. It is worth noting that the optimum predicted cooling rate (valley shown in Fig. 4b) might still be not conclusive due to the large variation in alloy composition tested and the error associated with the porosity measurement.

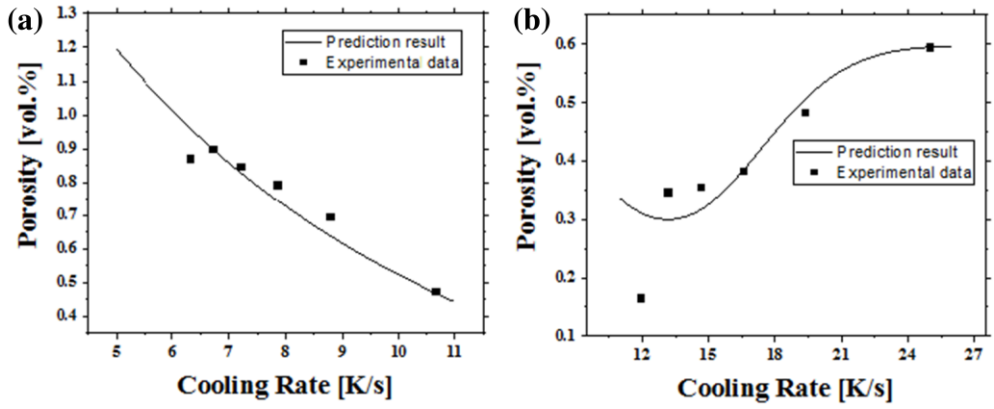

Figure 4 Predicted porosity and prior experimental data [7] as a function of cooling rate

Fig. 5 exhibits the GA-DE prediction for the variation of porosity as a function of alloy composition. It is clearly shown in Fig. 5a that porosity formation increases with increasing Fe content. This can be attributed to the formation of iron-containing β-intermetallics. The presence of these detrimental phase can increase the porosity content as they can cause flow blockage in the interdendritic channels [16, 17] and act as pore nucleation sites [13]. Silicon content has a small effect on the total porosity as seen in Fig. 5b. Previous work [7] have explored that Si can be beneficial to castability but could also promote porosity formation by forming intermetallic and eutectic phases. However, in this work, only slight change in porosity is observed with increasing Si content. Fig. 5c illustrates that higher level of Ti (i.e. more TiB_2 grain refiner) gives less porosity. This is because TiB_2 particles can provide active nucleation sites for pores, leading to more even distribution of small pores [18]. The reduction in porosity may also be related to the delayed dendrite coherency point of the grain-refined alloy [7]. The effect of Fe:Mn ratio of the alloy on pore formation is shown in Fig. 5d. More porosity is predicted with increasing Fe:Mn ratio. This is in a good agreement with previous experimental study which reported that the Fe:Mn ratio should be maintained at 2:1 to neutralize the effect of iron-containing β-intermetallics [19].

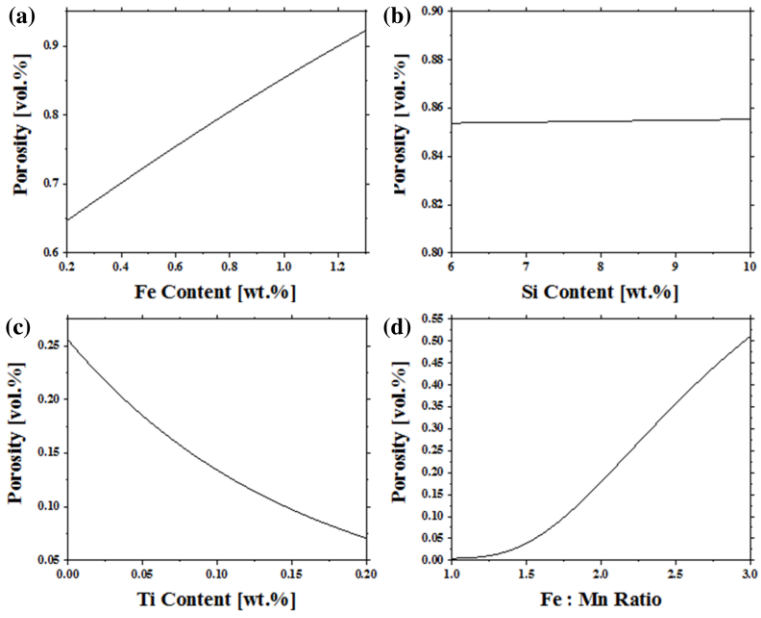

Figure 5 Contribution of alloy composition on percent porosity.

Conclusion

This research provides an alternative way for prediction of porosity formation in aluminium alloy casting by the application of evolutionary algorithms to generate predicting functions. The result function is capable of both the porosity percent prediction and the influence of compositions analysis. Because it provides the prediction results reasonably close to the ones in the training dataset and it also gives satisfying results after applying it to another dataset as well as the results from the influence of compositions analysis that agree with metallurgical theory. These abilities would allow industries to further optimize their production cost and time.

References

[1] Couper MJ, Neeson AE, Griffiths JR. Fatifue Fract Eng M 1990;13:213.
[2] Kubo K, Pehlke R. Metall Mater Trans B 1985;16:359.
[3] Lee PD, Chirazi A, See D. J Light Met 2001;1:15.
[4] Niyama E, Uchida T, Morikawa M, Saito S. AFS Int Cast Met J 1982;9:52.
[5] Shafyei A, Anijdan SHM, Bahrami A. Mat Sci Eng A 2006;431:206.
[6] Ghosh I, Das S, Chakraborty N. Neural Comput & Applic 2014;25:653.
[7] Dash M, Makhlouf M. J Light Met 2001;1:251.
[8] Whittenberger EJ, Rhines FN. Journal of Metals 1952:409.
[9] Paszkowicz W. Materials and Manufacturing Processes 2009;24:174.
[10] Storn R, Price K. J of Global Optimization 1997;11:341.
[11] Dinnis CM, Taylor JA, Dahle AK. Mat Sci Eng A 2006;425:286.
[12] Samuel AM, Pennors A, Villeneuve C, Samuel FH, Doty HW, Valtierra S. Int J Cast Met Res 2000;13:231.
[13] Roy N, Samuel A, Samuel F. Metall Mater Trans A 1996;27:415.
[14] Carlson KD, Lin Z, Beckermann C, Mazurkevich G, Schneider MC. In: Proceedings of Modeling of Casting, Welding and Advanced Solidification Processe (MCWASP). 2006. p.627.
[15] Hiromi N. Science and Technology of Advanced Materials 2001;2:49.
[16] Puncreobutr C, Phillion AB, Fife JL, Lee PD. Acta Mater 2014;64:316.
[17] Puncreobutr C, Lee PD, Kareh KM, Connolley T, Fife JL, Phillion AB. Acta Mater 2014;68:42.
[18] K.Tynelius, J.F.Major, D.Apelian. AFS Transactions 1993;101:401.
[19] Narayanan LA, Samuel FH. AFS Transactions 1992;100:383.